We are IntechOpen,
the world's leading publisher of
Open Access books
Built by scientists, for scientists

6,900
Open access books available

186,000
International authors and editors

200M
Downloads

Our authors are among the

154
Countries delivered to

TOP 1%
most cited scientists

12.2%
Contributors from top 500 universities

CLARIVATE ANALYTICS
BOOK CITATION INDEX
INDEXED

WEB OF SCIENCE™

Selection of our books indexed in the Book Citation Index
in Web of Science™ Core Collection (BKCI)

Interested in publishing with us?
Contact book.department@intechopen.com

Numbers displayed above are based on latest data collected.
For more information visit www.intechopen.com

Section-Map Stability Criterion for Biped Robots

Chenglong Fu, Zhao Liu and Ken Chen
Tsinghua University
China

1. Introduction

The importance of stability for dynamical systems is well-known. Any real system, including biped robots, need to be working under all kinds of disturbances. Whether the biped robot can effectively keep the planned motion under these disturbances is a fundamental property, and that is the explanation of stability intuitively. Stability of biped walking is the key problem in the theoretical framework of biped robots. Roughly speaking, the research of biped robots can be classified as the following three aspects: stability criterion, walking pattern planning, and walking pattern control. The purpose of stability criterion is to give the condition that the robot can realize stable walking under some control strategy. The purpose of walking pattern planning is to generate a desired gait offline or online, and it plays the role of feed-forward (Huang et al., 2001). The purpose of walking pattern control is to modify the planning walking pattern based on sensory information, and it plays the role of feedback (Huang & Nakamura, 2005). Among the above three aspects, stability criterion is the most fundamental and important, and it is the basis of walking pattern planning and real-time control. Although some researchers have proposed several walking control methods which are not based on stability criterion (Raibert, 1986; Geng et al., 2006); however if these methods can not ensure walking stability from the aspect of theory, then it will need many trials on hardware before success, and it is difficult to generate them to other platforms. Presently, there are the following three stability criteria for biped walking.

The first criterion is zero moment point (ZMP) criterion. The ZMP was originally defined as the point in the ground plane about which the net moments due to ground contacts become zero in the plane of ground (Vukobratovic & Juricic, 1969). As long as the ZMP lies strictly inside the support polygon of the foot, then the support foot will not rotate about its extremities, and the desired trajectories of the robot's joints are dynamically feasible, just like a stationary manipulator. Takanishi et al. (1985) and Hirai et al. (1998) have proposed the methods of pattern synthesis based on ZMP offline. Recently, Kajita et al. (2001), Lim et al. (2002), and Nishiwaki et al. (2002) discussed the methods of online pattern generation. The ZMP criterion is not a necessary condition for stable walking. The ZMP criterion results in a flat-footed and short-step walking style which is less dynamic than human beings. During normal walking, human do not always obeys the ZMP requirement and the foot does not always remain flat on the ground. Humans, even with prosthetic legs, use foot rotation to decrease energy loss at impact (Kuo, 2002). Based on the ZMP criterion, the robot can only realize static walking or quasi-dynamic walking, as shown in Fig. 1(a) and (b). During the dynamic walking of human beings, the under-actuated degree-of-freedom (DOF) emerges between the support foot and the ground, as shown in Fig.1 (c).
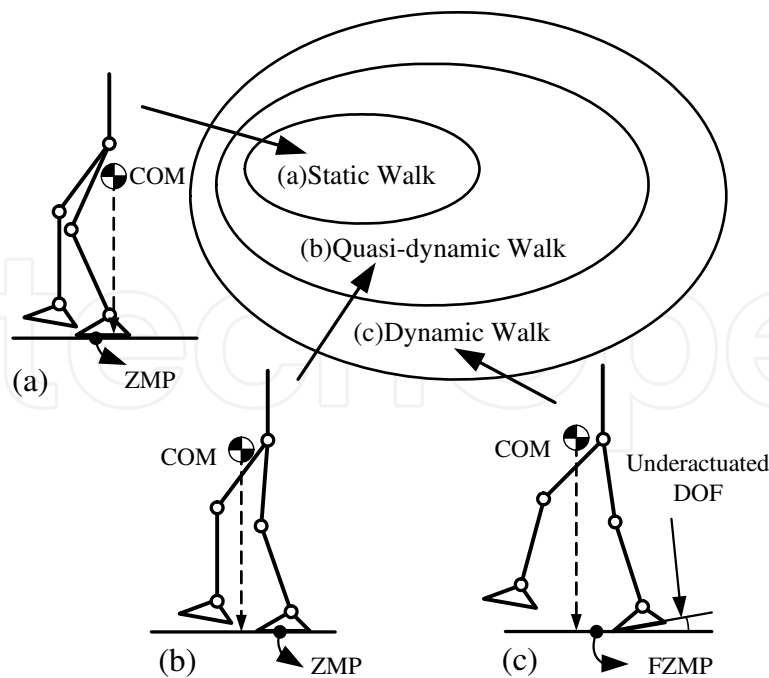
Fig. 1. Classification of biped locomotion. In case (a), the robot's nominal trajectory has been planned so that the center of mass (COM) and ZMP are both within the interior of the footprint. In case (b), COM has moved out of the footprint while ZMP still keeps within the interior of the footprint. In both case (a) and (b), the foot will not rotate, and thus the foot is acting as a base, just like a normal robotic manipulator. In case (c), however, both COM and ZMP has moved out the interior of the footprint, allowing the foot to rotate

The second stability criterion is Poincare return maps (Guckenheimer & Holmes, 1985), which is a technique for determining the existence of periodic orbits and their stability properties. With this method, the system is assumed to have a periodic limit cycle. Small deviations from the cycle follow the linear relation

$$X_{n+1} = KX_n \tag{1}$$

where X_n is the vector of deviations from the fixed point, K is a linear return map, and X_{n+1} is the vector of deviations in the following cycle. If the eigenvalues of K have moduli less than one, then the limit cycle is stable. Hurmuzlu and Moskowitz (1993) first applied the Poincare map to the locomotion systems, McGeer (1990) and Goswami et al. (1996) used this technique to analyze stability issues of passive walking robots. Grizzle et al. (2001) developed an extension of Poincare method that reduces the stability calculation to a one-dimensional map, and Westervelt et al. (2003a) used this method to design automated control for an under-actuated planar biped robot (Chevallereau et al., 2003). However, Using Poincare return maps as a stability criterion of biped walking has two serious limitations. Firstly, they are only applicable for periodic bipedal walking. There is nothing periodic about walking across unevenly spaces obstacles, or changing walking speed. Secondly, using eigenvalues of Poincare return maps is valid only for small deviations from a limit cycle. Large disruptions from a limit cycle, such as when being pushed, cannot be analyzed using this technique. Therefore, Poincare return maps are not necessary for analysing bipedal walking in general.

The third stability criterion is motivated by observation that human beings keep the relative small size of angular momentum about the center of mass (CoM) during walking. In the book Legged Robots that Balance, Raibert (1986) speculated that a control system that keeps angular momentum during stance could achieve higher efficiency and better performance. Popovic and Englehart (2004) have suggested that humanoid control systems should explicitly minimize global spin angular momentum during steady state forward walking. However, minimizing angular momentum is not a necessary condition for stable walking. Human can walk can walk while swinging his or her upper body which makes the global spin angular momentum larger than zero. Minimizing angular momentum is not a sufficient condition for stable walking, as a biped robot can fall down the ground while maintaining an angular zero momentum (Pratt & Tedrake, 2005). Therefore, angular momentum about the Center of Mass is not a good stability criterion for biped walking.

In fact, the desirable characteristics of an ideal stability criterion for biped walking may include:

1. Universal. The ideal stability criterion should be applicable not only to static walking, but also to dynamic walking. The ideal stability criterion should be applicable not only to periodic walking, but also to non-periodic walking.
2. Sufficient and Necessary. If the stability margin is outside an acceptable threshold of values, the robot will fall down. If the stability margin is inside an acceptable threshold of values, the robot will walk stably.
3. Comparable and Measurable. Two walking patterns should be comparable for stability based on their relative stability margins. One should be able to measure the relevant state variables and estimate the stability margin on-line in order to use it for control purposes (Pratt & Tedrake, 2005).
4. Simple and Convenient. The ideal stability criterion should be easy to compute, and convenient to be used in analyzing and controlling robots.

This chapter explores such a coherent stability criterion based on the description of biped walking from a global point of view. The organization of this chapter is organized as follows. Section II proposed an overall mathematical modeling method for biped walking is based on dimensional-variant hybrid automata. Section III presented a rigorous definition of biped walking stability by combining the character of biped locomotion with the notion of classical stability, and pointed out that the model in the task space is a length-varying and inertia-varying inverted pendulum. Section IV presented a stability criterion in task space of biped walking. Section V introduced application methods of the proposed criterion. Section VI provided the experimental results of a planar biped robot. Section VII concluded the chapter.

2. Overall mathematical model for dynamic biped walking
2.1 Assumption of dynamic walking

During biped locomotion, two legs alternately contact the ground. When only one leg contacts the ground, the robot is called in single support phase. When both legs contact the ground, the robot is called in double support phase. The overall biped walking consists of single support phase and double support phase.

In the field of biped locomotion, there's still no accurate and rigorous definition for dynamic walking (Goswami & Kallem, 2004). For the purposes of this chapter, to eliminate complications, we assume that dynamic walking should satisfy the following two requirements:

1. The under-actuated DOF emerges between the support foot and the ground during dynamic walking.

2. The double support phase is instantaneous and can be modeled as a rigid contact.

The robot is said to be in under-actuated phase when the robot is in the mode of toe or heel contact, and in fully-actuated phase when the robot is in the mode of full sole contact. A typical dynamic walking for biped robots with feet is shown in Fig.2.


(a) Foot contact   (b) Toe contact   (c) Heel contact   (d) Foot contact
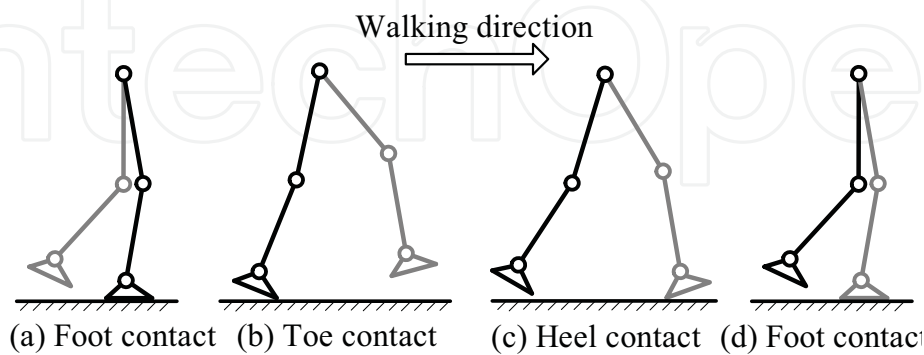
Fig. 2. A typical dynamic walking for biped robots with feet

Since the assumption of instantaneous double support phase, each discrete phase can be modeled as an N-link rigid body open-chain robot with one-DOF revolute joints. The equations of motion are given by the following general form:

$$D(q)\ddot{q} + C(q,\dot{q})\dot{q} + G(q) = Bu \tag{2}$$

where $q := (q_1; \cdots; q_N) \in Q$ are the joint angles, Q is a simply-connected, open subset of $[0, 2\pi)^N$ corresponding to physically reasonable configuration of the robot. The matrix $D(q)$ is the inertia matrix, the matrix $C(q)$ contains Coriolis and centrifugal terms, $G(q)$ is the gravity vector, and B is an input matrix.

Defining $x := (q; \dot{q})$, the model in each phase can be written in state space form

$$\dot{x} = \begin{bmatrix} \dot{q} \\ D^{-1}[-C\dot{q} - G] \end{bmatrix} + \begin{bmatrix} 0 \\ D^{-1}B \end{bmatrix} u =: f(x) + g(x)u \tag{3}$$

with state space $TQ := \{(q; \dot{q}) \mid q \in Q, \dot{q} \in R^N\}$.

2.2 Overall biped model based on dimension-variant hybrid automata

The overall biped model is hybrid and dimension-variant in nature, consisting of some continuous dynamics and re-initialization rules at the contact event. We propose an overall mathematical modeling method for biped walking based on dimension-variant hybrid automata. This method expresses the overall biped walking model as an 8-tuple

$$\mathbf{H} = (V, X, N, F, D, E, S, \Delta) \tag{4}$$

where

$V = \{foot, toe, heel, \cdots\}$ is the collection of discrete states;

$X = \{x_i : i \in V\}$ is the collection of continuous states;

$N = \{\dim(\boldsymbol{x}_i) : i \in V\}$ is the dimension of X ;

$F = \{F(i, \boldsymbol{x}) : V \times X \to TX\}$ is the vector fields;

$D = \{TQ_i : i \in V\}$ is the collection of domains;

$E \subseteq V \times V$ is the collection of edges;

$S = \{S_e : e \in E\}$ is the collection of transition sections;

$\Delta = \{\Delta_e : e \in E\}$ is the collection of transition rules;

Let $(\cdot)^-$ and $(\cdot)^+$ donate quantities immediately just before and after transition. Given $\mathbf{H}$, the basic idea is that starting from a point in some domain TQ_i, we flow according to F_i until (and if) we reach some transition section S_i^j, then switch via the transition rule Δ_i^j, continue flowing in TQ_j, according to F_j and so on, as shown in Fig. 3.
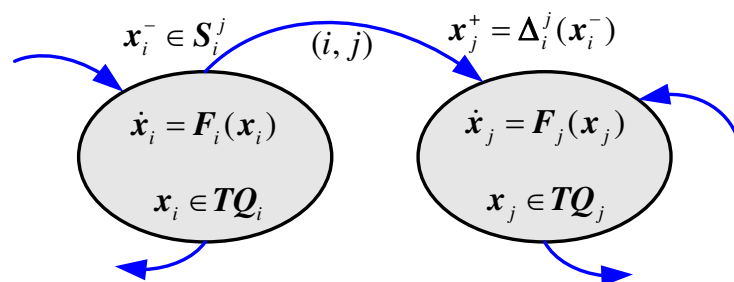

Fig. 3. Diagram of dimension-variant hybrid automata

A typical dynamic walking with feet shown in Fig.2 can be modeled as a dimension-variant hybrid automaton, as shown in Fig. 4. This modelling method can reflect all kinds of continuous and discrete properties of biped walking, which makes it possible to study stability and design control strategy for biped locomotion from a global point of view.

It should be noted that the solution $\boldsymbol{\varphi}^t(\boldsymbol{x}_0)$ of dimension-variant hybrid automata is piecewise continuous and hybrid, as shown in Fig.5.

3. Stability definition and task space

3.1 Stability definition of biped walking

The manuscript has to be submitted in MS Word (*.doc) and PDF format. If you use other word editors and can not transfer it in Word and PDF please contact us. The most intuitive definition of biped stability is likely that "the biped does not fall". This section will give a sequence of preliminary definitions leading to a rigorous mathematical definition of biped walking stability by combining the character of biped locomotion with the notion of classical stability from the view of hybrid automata.

Since the main destination of biped walking is to avoid fall, following (Pratt & Tedrake, 2005), we define a fall in this chapter as follows.

Definition 4.1 (Fall) Let Q_{Fall} be a set of the robot's configuration in which a point on the biped, other than a point on the feet, touches the ground.

There are three modes of fall for biped robots considering in this chapter as shown in Fig. 6. Let $\boldsymbol{q}$ and $\dot{\boldsymbol{q}}$ denote the vector of generalized position and velocity respectively. $\boldsymbol{Q}_{\text{Fall}}$ can be expressed as

$$\boldsymbol{Q}_{\text{Fall}} = \{\boldsymbol{q} \mid y_{\text{torso}}(\boldsymbol{q}) = 0\} \cup \{\boldsymbol{q} \mid y_{\text{hip}}(\boldsymbol{q}) = 0\} \cup \{y_{\text{knee}}(\boldsymbol{q}) = 0\} \tag{5}$$
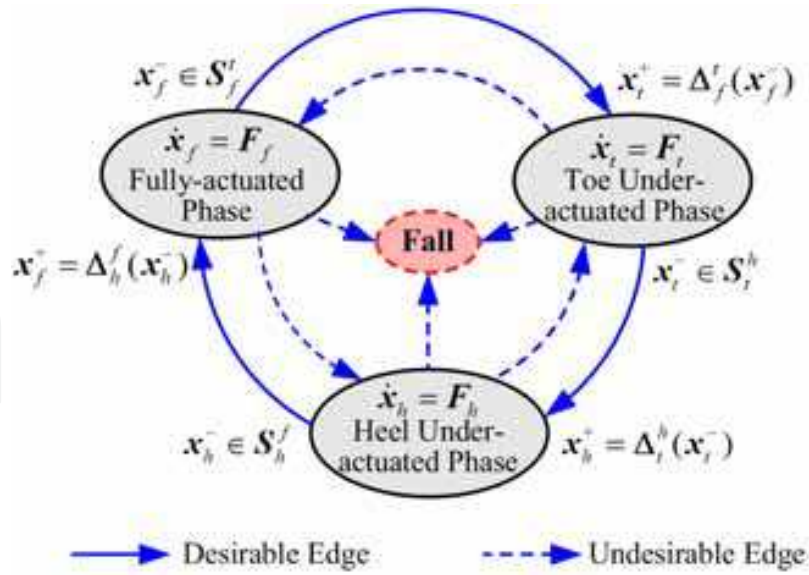
Fig. 4. Dimension-variant hybrid automata for dynamic walking wirh feet

Fig. 5. Solution of dimension-variant hybrid automata

(a) Torso mode   (b) Hip mode   (c) Knee mode
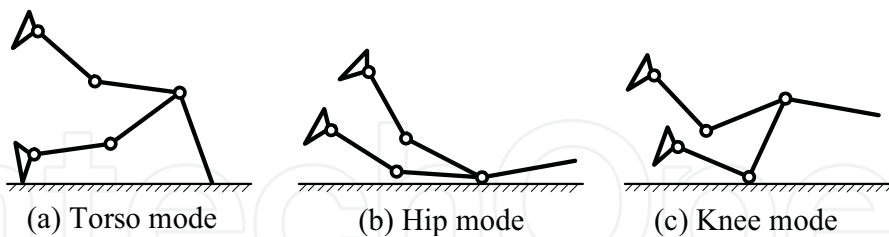
Fig. 6. Three modes of fall configuration

Introducing the state vector $x = (q; \dot{q})$, the solution starting from x_0 can be donated as $\varphi^t(x_0)$, and it is hybrid and piecewise continuous. Let $\mathbf{Orb}(x_0) = \{\varphi^t(x_0) \mid 0 \le t < \infty\}$ donate the hybrid orbit of biped walking. It should be noted that $\mathbf{Orb}(x_0)$ can be not only periodic walking (Gizzle et al., 2001), but also non-periodic walking.

Definition 4.2 (Feasible Orbit) Let $\mathbf{Orb}(x_0)$ be a hybrid orbit starting from x_0. If $\forall (q; \dot{q}) \in \mathbf{Orb}(x_0)$, satisfying

$$q \notin Q_{\text{Fall}} \tag{6}$$

then $\mathbf{Orb}(x_0)$ is a feasible orbit.

Definition 4.3 (Distance between a Point and an Orbit) Given a norm $||\cdot||$, the distance between a point $x_i \in TQ_i$ and an orbit $\mathbf{Orb}(x_0)$ can be defined as

$$\text{dist}(x_i, \mathbf{Orb}(x_0)) := \inf_{y \in \mathbf{Orb}(x_0) \cap TQ_i} ||x_i - y|| \tag{7}$$

Definition 4.4 (Open Neighborhood of an Orbit) Let $\mathbf{Orb}(x_0)$ be an orbit starting from x_0. Given a norm $||\cdot||$, the open neighborhood of an orbit $\mathbf{Orb}(x_0)$ can be defined as

$$\Omega_\delta(\mathbf{Orb}(x_0)) = \{x \mid \text{dist}(x, \mathbf{Orb}(x_0)) < \delta\} \tag{8}$$

Definition 4.5 (Stable Walking) Let $\mathbf{Orb}(x_0)$ be a feasible orbit of biped walking. If $\forall \varepsilon > 0$, $\exists \delta(\varepsilon) > 0$ which determines an open neighbourhood $\Omega_\delta(\mathbf{Orb}(x_0))$ such that for every $x \in \Omega_\delta(\mathbf{Orb}(x_0))$, satisfying $\varphi^t(x) \in \Omega_\varepsilon(\mathbf{Orb}(x_0))$ for all $t \geq 0$, then the biped walking is stable.

Definition 4.6 (Attractive Walking) Let $\mathbf{Orb}(x_0)$ be a feasible orbit of biped walking. If $\exists \delta > 0$ which determines an open neighbourhood $\Omega_\delta(\mathbf{Orb}(x_0))$ such that for every $x \in \Omega_\delta(\mathbf{Orb}(x_0))$, satisfying $\lim_{t \to \infty} \varphi^t(x) \in \mathbf{Orb}(x_0)$, then the biped walking is attractive.

Definition 4.7 (Asymptotically Stable Walking) If a biped walking is both stable and attractive, then it is asymptotically stable.

Definition 4.8 (Exponentially Stable Walking) If there exists $\delta > 0$, $\gamma > 0$, and $\beta > 0$ such that, $\forall t > 0$,

$$\text{dist}(\varphi^t(x), \mathbf{Orb}(x_0)) \leq \gamma e^{-\beta t} \text{dist}(x, \mathbf{Orb}(x_0)) \tag{9}$$

whenever $x \in \Omega_\delta(\mathbf{Orb}(x_0))$.

3.2 Biped model in the task space

The definition of biped stability is established in high-DOF space; however it is difficult to study the stability in this high-DOF space directly. Although biped robots are typically high DOF mechanisms, the task of biped walking is inherent a low DOF task. Considering planar biped walking, the task space is only 1-DOF problem, as shown in Fig. 7.

In fact, stability of biped walking can be studied in the low-DOF task space under virtual constraint control strategy (Gizzle et al., 2001; Canudas-de-Wit, 2004), as shown in Fig. 8.

Inspired by the work of Westervelt et al. (2003a), let θ and σ donate the position and angular momentum around the pivot point of the stance leg respectively. Let $z_i = (\theta_i; \sigma_i) \in Z_i \subset \mathbb{R}^2$ donate the state variable of the task space. According to the angular momentum balance theorem, the model of the task space has the following special form
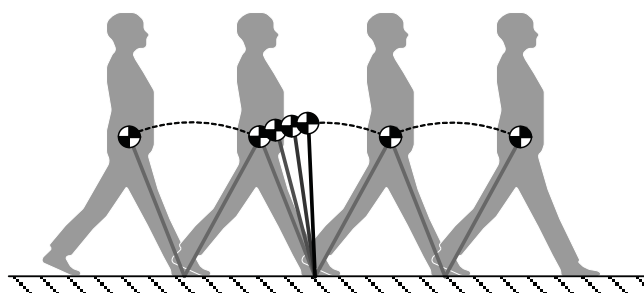

Fig. 7. Task Space of biped locomotion in sagittal plane
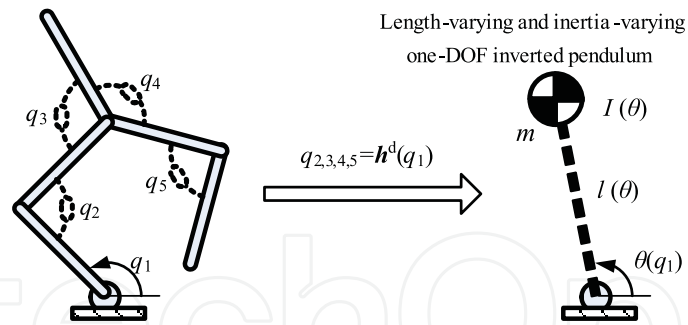
Fig. 8. Example of virtually constrainted system

$$\begin{pmatrix} \dot{\theta}_i \\ \dot{\sigma}_i \end{pmatrix} = \begin{pmatrix} \dfrac{\sigma_i}{I_i(\theta_i)} \\ J_i(\theta_i) \end{pmatrix} \tag{10}$$

where I_i plays the role of an inertia, and J_i plays the role of a net moment around the pivot.

3.3 Basic definitions for the biped model in the task space

Let $F_i(\theta_i, \sigma_i) := \begin{pmatrix} \dfrac{\sigma_i}{I_i(\theta_i)} \\ J_i(\theta_i) \end{pmatrix}$ donate the vector field in task space. We assume the following

conditions are satisfied:

   H1) $Z_i \subset \mathbb{R}^2$ is open and connected;

   H2) $F_i : Z_i \to \mathbb{R}^2$ is C^1;

   H3) A solution $\varphi^t(z_i)$ is right continuous on t, and depends continuously on the initial condition z_i;

   H4) Transition section is designed as $S_i^{i+1} = \{(\theta_i, \sigma_i) \mid \theta_i = \theta_i^-\}$

   H5) v is C^1, and $\Delta_i^{i+1}(S_i^{i+1}) \cap S_i^{i+1} = \varnothing$;

   H6) $\sigma_i > 0$ during normal forward walking.

Definition 4.9 (Time Function) $T : Z_i \to \mathbb{R}$ is defined as

$$T(z_i) := \{t \geq 0 \mid \varphi^t(z_i) \in S_i^{i+1}\} \tag{11}$$

The meaning of time function is the time to the transition section at the first time.

Definition 4.10 (Distance Function) $d : Z_i \to \mathbb{R}$ is defined as

$$d(z_i) := \sup_{0 \leq t < T(z_i)} \text{dist}(\varphi^t(z_i), \mathbf{Orb}(z_0^*)) \tag{12}$$

The meaning of distance function is the maximum distance between $\mathbf{Orb}(z_0^*)$ and solution $\varphi^t(z_i)$ before the first time to impact section.

Definition 4.11 (Total Distance Function) $D : Z_i \to \mathbb{R}$ is defined as

$$D(z_i) := \sup_{0 \le t < \infty} \text{dist}(\boldsymbol{\varphi}^t(z_i), \mathbf{Orb}(z_0^*)) \tag{}$$

The meaning of distance function is the maximum distance between $\mathbf{Orb}(z_0^*)$ and solution $\boldsymbol{\varphi}^t(z_i)$ while $t \in (0, \infty]$.

Lemma 1: [(Grizzle, 2001), Lemma3 and 4] Suppose that H1-H4 hold, then $T(z_i)$ and $d(z_i)$ is continuous.

Lemma 2: Suppose that H1-H5 hold, then $D(z_i)$ is continuous.

Proof: According to the definition of total distance function, $D(z_i)$ can be written as

$$D(z_i) = \sup\{d(z_i), \ d(z_{i+1}^+), \ d(z_{i+2}^+), \ \cdots\} \tag{14}$$

where $d(z_{i+1}^+) = d \circ \Delta_i^{i+1} \circ \lim_{t \to T(z_i)} \boldsymbol{\varphi}^t(z_i)$. By H3), H5), and Lemma 2, $d(z_{i+1}^+)$ is continuous. In the same way, any item in the right side of the equation (14) is continuous. Therefore, $D(z_i)$ is continuous. ♠

4. Stability criterion in the task space

4.1 Section Sequence and its Stability Equivalence to Orbit

Definition 5.1 (Section Sequence) $\{\bar{z}_i^*\}_{i=0}^{\infty}$ is defined as a set of intersection point between $\mathbf{Orb}(z_0^*)$ and transition sections as shown in Fig. 9, and $\bar{z}_i^*$ can be written as

$$\bar{z}_i^* := \overline{\mathbf{Orb}}(z_0^*) \bigcap S_i^{i+1} \tag{15}$$

where $\overline{\mathbf{Orb}}(z_0^*)$ is the set closure of $\mathbf{Orb}(z_0^*)$.
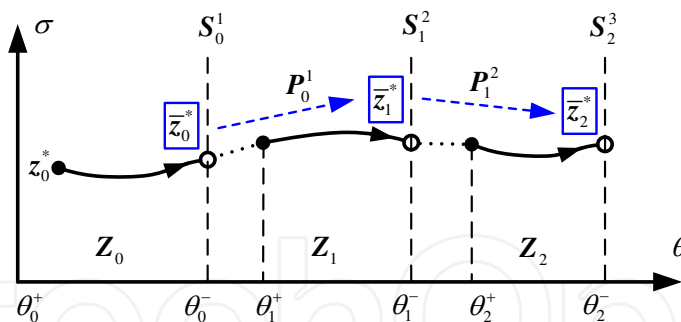
Fig. 9. Section sequence and section map

Theorem 1 Under H1)–H5), if section sequence $\{\bar{z}_i^*\}_{i=0}^{\infty}$ is stable (resp., asymptotically stable, or exponentially stable), orbit $\mathbf{Orb}(z_0^*)$ is stable (resp., asymptotically stable, or exponentially stable).

Proof: The process can be summed up into the following three parts:

1. Proving stable

Since section sequence $\{\bar{z}_i^*\}_{i=0}^{\infty}$ is stable, then $\forall \bar{\varepsilon} > 0$, $\exists \bar{\delta}(\bar{\varepsilon}) > 0$ such that for every $\bar{z}_0 \in \boldsymbol{B}_{\bar{\delta}(\bar{\varepsilon})}(\bar{z}_0^*)$, satisfying $\bar{z}_i \in \boldsymbol{B}_{\bar{\varepsilon}}(\bar{z}_i^*)$ for all $i \ge 0$. This implies that $\forall \bar{z}_0 \in \boldsymbol{B}_{\bar{\delta}(\bar{\varepsilon})}(\bar{z}_0^*)$, there exists a solution $\boldsymbol{\varphi}^t(z_0)$ defined on $[0, \infty)$ with the initial value z_0. Moreover, following [(Grizzle, 2001), Equation (55)], an upper bound on how far the solution $\boldsymbol{\varphi}^t(z_0)$ wanders from the orbit is given by

$$\sup_{t\geq 0}\text{dist}(\boldsymbol{\varphi}^t(z_0),\textbf{Orb}(z_0^*)) \leq \sup_{z\in\boldsymbol{\Omega}_{\bar{\varepsilon}}(\overline{\textbf{Orb}}(z_0^*))\cap S}\text{D}(z) \tag{16}$$

According to Lemma 2, $\text{D}(z_i)$ is continuous; moreover, for $z\in\overline{\textbf{Orb}}(z_0^*)\cap S$, $\text{D}(z)=0$. This implies that $\forall\varepsilon>0$, $\exists\bar{\varepsilon}>0$, satisfying

$$\sup_{z\in\boldsymbol{\Omega}_{\bar{\varepsilon}}(\overline{\textbf{Orb}}(z_0^*))\cap S}\text{D}(z)<\varepsilon \tag{17}$$

Take (17) into (16), and yield

$$\sup_{t\geq 0}\text{dist}(\boldsymbol{\varphi}^t(z_0),\textbf{Orb}(z_0^*))<\varepsilon \tag{18}$$

According to definition 4.4, (18) can be written as

$$\boldsymbol{\varphi}^t(z_0)\in\boldsymbol{\Omega}_\varepsilon(\textbf{Orb}(z_0^*)) \tag{19}$$

By H3) and H4), It is easy to construct a small enough open neighborhood $\boldsymbol{\Omega}_\delta(\textbf{Orb}(z_0^*))$ satisfying that when $z\in\boldsymbol{\Omega}_\delta(\textbf{Orb}(z_0^*))\cap Z_0$, $\bar{z}_0\in\boldsymbol{B}_{\bar{\delta}}(\bar{z}_0^*)$, which proves that the orbit is stable

2.   Proving asymptotic stable

Since section sequence $\{\bar{z}_i^*\}_{i=0}^\infty$ is asymptotically stable, then there exists $\delta>0$ such that for every $\bar{z}_0\in\boldsymbol{B}_{\bar{\delta}(\bar{\varepsilon})}(\bar{z}_0^*)$, satisfying $\lim_{i\to\infty}\bar{z}_i\in\overline{\textbf{Orb}}(z_0^*)$. According to definition 4.3, we have $\lim_{i\to\infty}\text{D}(\bar{z}_i)=0$. This implies that there exists a solution $\boldsymbol{\varphi}^t(z_0)$ satisfying $\lim_{t\to\infty}\text{dist}(\boldsymbol{\varphi}^t(z_0),\textbf{Orb}(z_0^*))=0$, which proves that the orbit is asymptotically stable.

3.   Proving exponentially stable

Since section sequence $\{\bar{z}_i^*\}_{i=0}^\infty$ is exponentially stable, then there exists $\delta>0$, $\gamma>0$ and $\beta>0$ such that, for all $i\geq 0$,

$$||\bar{z}_i-\bar{z}_i^*||\leq\gamma e^{-\beta i}||\bar{z}_0-\bar{z}_0^*|| \tag{20}$$

whenever $\bar{z}_0\in\boldsymbol{\Omega}_\delta(\overline{\textbf{Orb}}(z_0^*))\cap S_0^1$

According to Lemma 1 and H5), for any $i\geq 0$, $\text{T}(z_i)$ and $\Delta_i^{i+1}(\bar{z}_i)$ are all continuous; therefore, there exists an open ball $\boldsymbol{B}_r(\bar{z}_i^*)$, $\text{T}_{min}>0$, $\text{T}_{max}>0$, such that for $\bar{z}_i\in\boldsymbol{B}_r(\bar{z}_i^*)\cap S_i^{i+1}$,

$$0<\text{T}_{min}\leq\text{T}\circ\Delta_i^{i+1}(\bar{z}_i)\leq\text{T}_{max}<\infty \tag{21}$$

Since exponential stability of $\{\bar{z}_i^*\}_{i=0}^\infty$ implies stability of $\{\bar{z}_i^*\}_{i=0}^\infty$, $\textbf{Orb}(z_0^*)$ is also stable. Thereby, there exists $\delta>0$, such that for $z_0\in\boldsymbol{\Omega}_\delta(\textbf{Orb}(z_0^*))$, satisfying $\boldsymbol{\varphi}^t(z_0)\in\boldsymbol{\Omega}_r(\textbf{Orb}(z_0^*))$ for all $t\geq 0$. According to H3), H4) and standard bounds for the Lipschitz dependence of the solution w.r.t. its initial condition, it follows that for $\bar{z}_i\in\boldsymbol{B}_\delta(\bar{z}_i^*)\cap S_i^{i+1}$,

$$\sup_{0\leq t\leq\text{T}\circ\Delta_i^{i+1}(\bar{z}_i)}\text{dist}(\boldsymbol{\varphi}^t\circ\Delta_i^{i+1}(\bar{z}_i),\textbf{Orb}(z_0^*))\leq\sup_{0\leq t\leq\text{T}_{max}}||\boldsymbol{\varphi}^t\circ\Delta_i^{i+1}(\bar{z}_i)-\boldsymbol{\varphi}^t\circ\Delta_i^{i+1}(\bar{z}_i^*)||\leq L_i||\bar{z}_i-\bar{z}_i^*|| \tag{22}$$

where L_i is the Lipschitz constant of continuous function $\boldsymbol{\varphi}^t\circ\Delta_i^{i+1}(\cdot)$.

According to (20) and (22), for $i\geq 0$,

$$\sup_{0\leq t\leq\text{T}\circ\Delta_i^{i+1}(\bar{z}_i)}\text{dist}(\boldsymbol{\varphi}^t\circ\Delta_i^{i+1}(\bar{z}_i),\textbf{Orb}(z_0^*))\leq L_i\gamma e^{-\beta i}||\bar{z}_0-\bar{z}_0^*|| \tag{23}$$

Define $L = \sup_i L_i$, and considering (21) and (23), for all $t \geq 0$,

$$\text{dist}(\boldsymbol{\varphi}^t(z_0), \mathbf{Orb}(z_0^*)) \leq L\gamma e^{\beta} \cdot e^{-\frac{\beta}{T_{\max}}t} \mid\mid \overline{z}_0 - \overline{z}_0^* \mid\mid \tag{24}$$

By H3) and H4), there exists $c > 0$ such that

$$\mid\mid \overline{z}_0 - \overline{z}_0^* \mid\mid \leq c \cdot \text{dist}(z_0, \mathbf{Orb}(z_0^*)) \tag{25}$$

The proof of asymptotical stability can be finished by taking (25) into (24).

4.2 Section map and its analytical form

Definition 5.2 (Section Map) $P_i^{i+1} : S_i^{i+1} \cap Z_i \to S_{i+1}^{i+2} \cap Z_{i+1}$ is defined as

$$P_i^{i+1}(\overline{z}_i^*) := \varphi^{T(\Delta(\overline{z}_i^*))}(\Delta(\overline{z}_i^*)) \tag{26}$$

The meaning of section map is the map between two contiguous section sequences, as shown in Fig. 9.

Remark 1: It should be noted that section map does not need the system is periodic.

Since Z_i is two-dimensional, $S_i^{i+1} = \{(\theta_i; \sigma_i) \mid \theta_i = \theta_i^-\}$ is a one-dimensional restriction; therefore, section map and section sequence are both one-dimensional essentially. By H6), $\rho_i^{i+1} : (\sigma_i^-)^2 \to (\sigma_{i+1}^-)^2$ is homeomorphous with P_i^{i+1}, and section map $\{\sigma_i^-\}_{i=0}^\infty$ is homeomorphous to $\{(\sigma_i^-)^2\}_{i=0}^\infty$, which can be written as

$$\{(\sigma_i^-)^2\}_{i=0}^\infty = \{\rho_{i-1}^i \circ \cdots \circ \rho_0^1((\sigma_0^-)^2)\}_{i=0}^\infty \tag{27}$$

Thereby, the stability of section sequence is determined by the form of ρ_i^{i+1}.

By (10), section map $\rho_{i-1}^i : (\sigma_{i-1}^-)^2 \to (\sigma_i^-)^2$ can be written as

$$(\sigma_i^-)^2 = (\delta_{i-1}^i \cdot \sigma_{i-1}^-)^2 + 2\int_{\theta_i^+}^{\theta_i^-} I_i(\theta_i) J_i(\theta_i) d\theta_i \tag{28}$$

where $\delta_{i-1}^i := \sigma_i^+ / \sigma_{i-1}^-$ is called section-map factor.

It should be noted that (28) is a one-dimensional linear time-invariant map.

4.3 Section-map stability criterion

Theorem 2 (Section-map Stability Criterion) Under H1)–H6), if $0 < \sup_{i>0} \delta_{i-1}^i < 1$, $\mathbf{Orb}(z_0^*)$ is exponentially stable; moreover, the smaller $\sup_{i>0} \delta_{i-1}^i$ is, the faster $\mathbf{Orb}(z_0^*)$ converges.

Proof: According to Theorem 1, the exponential stability of $\mathbf{Orb}(z_0^*)$ lies on the exponential stability of $\{\overline{z}_k^*\}_{k=0}^\infty$. Since $\{\overline{z}_k^*\}_{k=0}^\infty$ and $\{(\sigma_i^-)^2\}_{i=0}^\infty$ is homeomorphous, the following will prove the exponential stability of $\{(\sigma_i^-)^2\}_{i=0}^\infty$.

Define $\xi_i = (\sigma_i^-)^2$, and $\{\xi_i^*\}_{i=0}^\infty$ can be written as

$$\{\xi_i^*\}_{i=0}^\infty = \{\xi_0^*, \ \rho_0^1(\xi_0^*), \ \rho_1^2 \circ \rho_0^1(\xi_0^*), \ \cdots, \ \rho_{i-1}^i \circ \cdots \circ \rho_0^1(\xi_0^*), \ \cdots\} \tag{29}$$

When there exists an initial perturbation $\mid\mid \xi_0 - \xi_0^* \mid\mid < \delta$, according to (28), for all $i \geq 0$,

$$||\xi_i - \xi_i^*|| = ||\rho_{i-1}^i(\xi_{i-1}) - \rho_{i-1}^i(\xi_{i-1}^*)|| = (\delta_{i-1}^i)^2 ||\xi_{i-1} - \xi_{i-1}^*|| = (\delta_{i-1}^i)^2 \cdots (\delta_0^1)^2 \cdot ||\xi_0 - \xi_0^*|| \quad (30)$$

Moreover,

$$(\delta_{i-1}^i)^2 \cdots (\delta_0^1)^2 \le (\delta_{max})^{2i} = (e^{\ln \delta_{max}})^{2i} = e^{2(\ln \delta_{max}) \cdot i} \quad (31)$$

Take (31) into (30), and yield

$$||\xi_i - \xi_i^*|| \le e^{2(\ln \delta_{max}) \cdot i} ||\xi_0 - \xi_0^*|| \quad (32)$$

Since $0 < \sup_{i>0} \delta_{i-1}^i < 1$, then $\ln(\sup_{i>0} \delta_{i-1}^i) < 0$, which proves that $\{\xi_i^*\}_{i=0}^{\infty}$ is exponential stable. ♠

Remark 2: Theorem 2 can be intuitively explained as: If the error arising from an initial perturbation can be shrinked at each impact, then the stability of the orbit can be achieved, vice versa, as shown in Fig. 10.
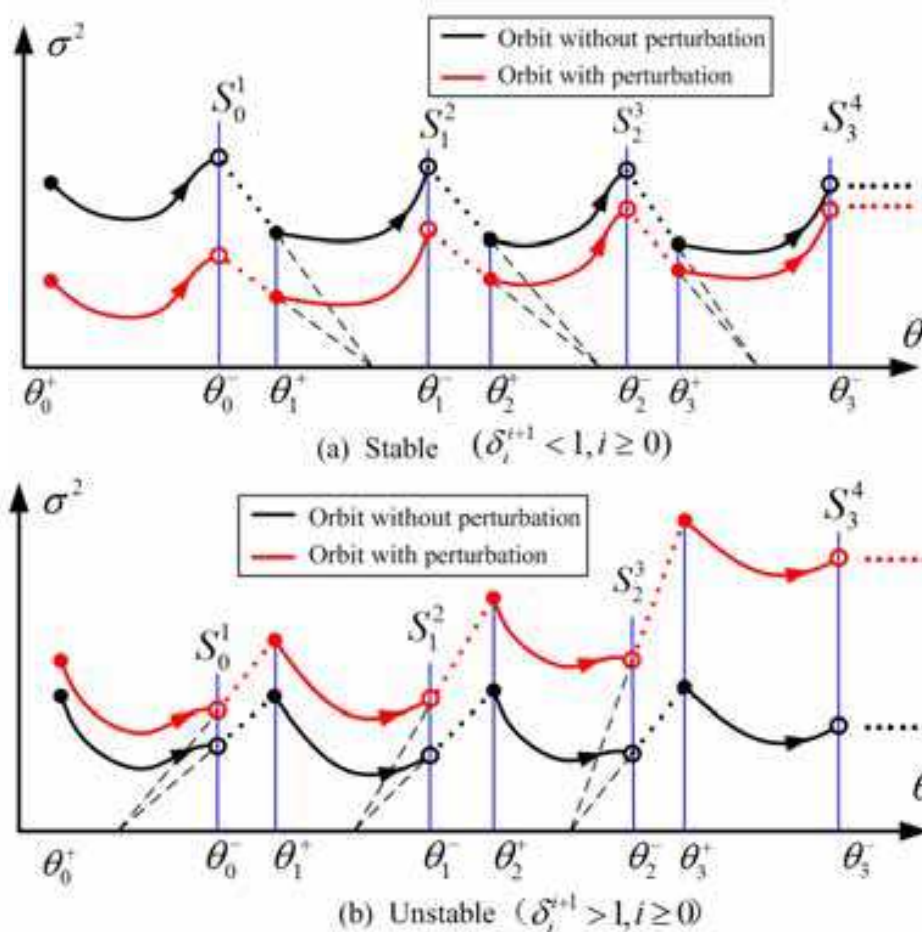
Fig. 10. Intuitive explaination of section-map stability criterion

Remark 3: Section-map Stability Criterion is an extension of Poincare return maps, and it is applicable to non-periodic walking which Poincare return map criterion can not solve.

In Section I, we have asserted that a desirable stability criterion for biped walking should satisfy four characteristics. In followings, we will give an explanation for section-map stability criterion about the above four characteristics.

1. **Universal.** Section-map stability criterion is established on a rigorous definition of biped walking; therefore it can not only be applicable to static walking, but also to dynamic walking, and can not only be used to study periodic walking, but also to non-periodic walking.

2. **Necessary and Sufficient.** Section-map stability criterion is a sufficient condition for biped walking, is a necessary condition for periodic walking, and is a quasi-necessary condition for non-periodic walking. The quasi-necessary condition means that the condition that all section-map factors are less than one is not necessary for non-periodic walking, but the number of section-map factors which is less than one should be larger than the number of section-map factors which is more than one.

3. **Comparable and Measurable.** By comparing the section-map factors of two walking patterns, one can determine which pattern is more stable. The lower δ, the faster the convergence toward the reference trajectory after perturbation. One can measure the relevant state variables and calculate or estimate the stability margin on-line in order to use it for control purposes.

4. **Simple and Convenient.** Comparing with ZMP criterion, it is not necessary to calculate all points of trajectories, and only transition points need to be calculated. Comparing with Poincare methods, the proposed criterion study biped walking in low-dimension task space and has a concise form; therefore section-map stability criterion is easy to compute, and convenient to be used in analyzing and controlling biped walking.

5. Applications of section-map stability criterion to planar biped walking

5.1 Planar biped robot THR-I
To test the validation of the proposed criterion, a planar biped robot called THR-I has been developed, and this robot has five links which are connected by revolute joints. To constrain motions in the frontal plane, THR-I was constructed with a boom attached at the hip joint, as shown in Fig. 11. The boom constrains the sagittal plane to be tangent to a sphere centered at the universal joint, and still allows the robot to freely trip or fall forward or backward. The material of the boom is made of carbon fiber which is rather light, and the length of the boom is more than 5 times leg length of THR-I; therefore, the influence of the boom on THR-I' dynamics in the sagittal plane is very small.
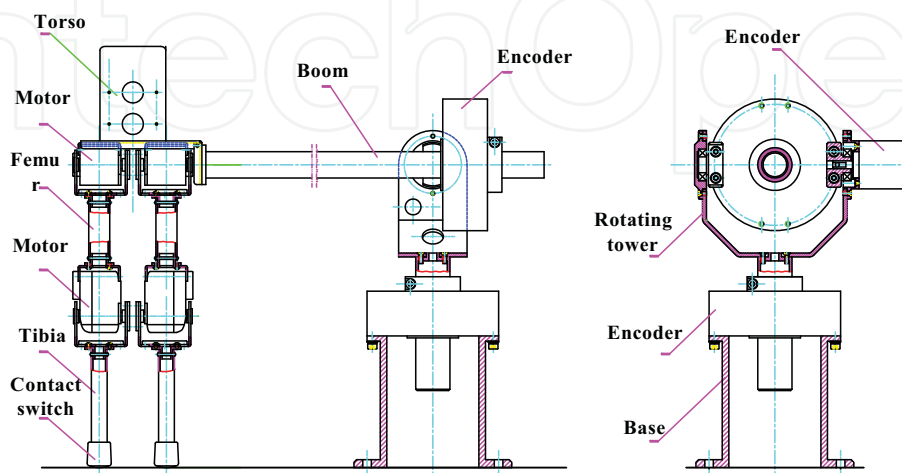

Fig. 11. Mechanical structure of THR-I.

Encoders are located between the boom and hip joint, and binary contact switches are located at the tip of the leg to detect whether or not a leg is in contact with the walking surface. There is no actuation at the stance leg tip. Hence, the robot is underactuated. It is assumed that walking consists of two successive phase: a single support phase and an instantaneous impact phase. Although this robot is simple, it captures the main difficulties: hybrid, static instability, and under-actuation. This model was also adopted in (Geng et al., 2006; Chevallereau et al., 2003).

To describe the shape of the biped, let $q_c = (q_1, q_2, q_3, q_4)'$ denote the configuration coordinates, and q_5 denote the absolute coordinate of the torso with respect to the coordinate frame as shown in Fig.12. The vector of the generalized coordinates of the biped robot is defined as $q = (q_1, q_2, q_3, q_4, q_5)'$. Let (x_{com}, y_{com}) denote the Cartesian coordinates of the center of mass. Torques u_i, $i = 1$ to 4, are applied between each connection of two links. Let σ denote the biped angular momentum around the pivot point of the stance leg. For the above choice of the coordinates in the support phase, σ has the following form (Chevallereau, 2004):

$$\sigma = -D_5(q_c)\dot{q} \tag{33}$$

where $D_5(q_c)$ is the fifth line of matrix $D(q_c)$.
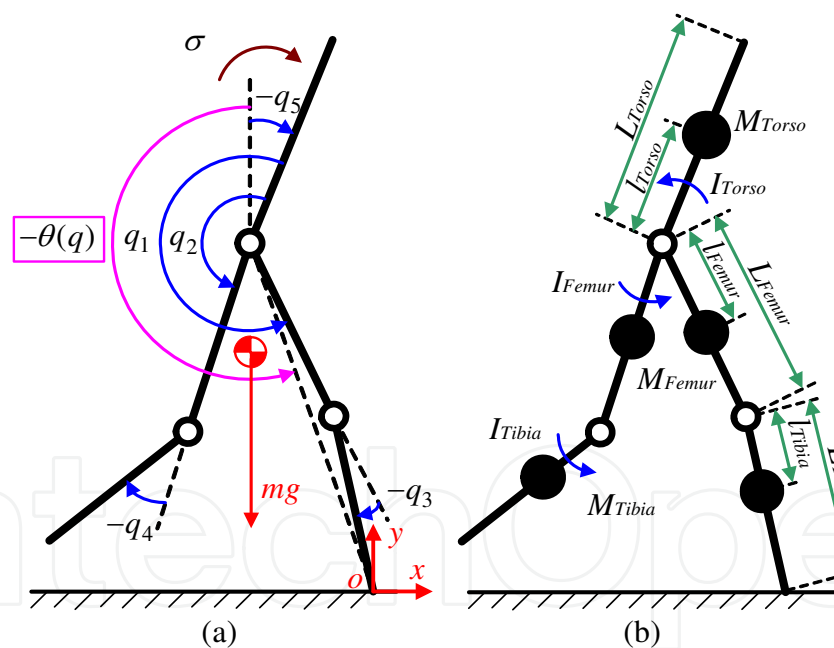
Fig. 12. Model of a 5-link THR-I biped robot

Since only the gravity affects the angular momentum around the pivot point, the angular momentum dynamics can therefore be written as

$$\dot{\sigma} = mg \cdot x_{com}(q) \tag{34}$$

Let q^-, q^+, $\dot{q}^-$, and $\dot{q}^+$ denote the pre- and post-impact generalized positions and generalized velocities, respectively. The superscript "−" and "+" will denote quantities immediately before and after impact thereinafter.

We assumed that the impact is instantaneous and inelastic. After impact the former stance leg is lifted off immediately, and the legs swap roles, which can be written as the following transformation equation:

$$q^+ = Rq^-$$
(35)

where $R = \begin{bmatrix} 0 & 1 & 0 & 0 & 0 \\ 1 & 0 & 0 & 0 & 0 \\ 0 & 0 & 0 & 1 & 0 \\ 0 & 0 & 1 & 0 & 0 \\ 0 & 0 & 0 & 0 & 1 \end{bmatrix}$ is a circular matrix describing the exchange of the support leg.

According to the conservation of momentum about impact point and no rebound nor slip at impact of swing leg tip, the map from $\dot{q}^-$ and $\dot{q}^+$ can be obtained respectively by

$$\dot{q}^+ = \Delta_{\dot{q}}(q^-)\dot{q}^-$$
(36)

where $\Delta_{\dot{q}}(q^-)$ can be found in (Westervelt et al., 2003a).

5.2 Synthesizing periodic walking patterns based on section-map factor

Consider the following output function (Westervelt et al., 2003a):

$$y = h(q) := h_0(q) - h_d \circ \theta(q)$$
(37)

where $h_0(q)$ specifies the four actuated joints that are to be controlled and $h_d \circ \theta(q)$ specifies the desired evolution of these joints as a function of the monotonic quantity θ(q), as shown in Fig. 13. Driving y to zero will force $h_0(q)$ to track $h_d \circ \theta(q)$; thus the configuration of the robot is being controlled as a holonomic constraint parameterized by $\theta(q)$.
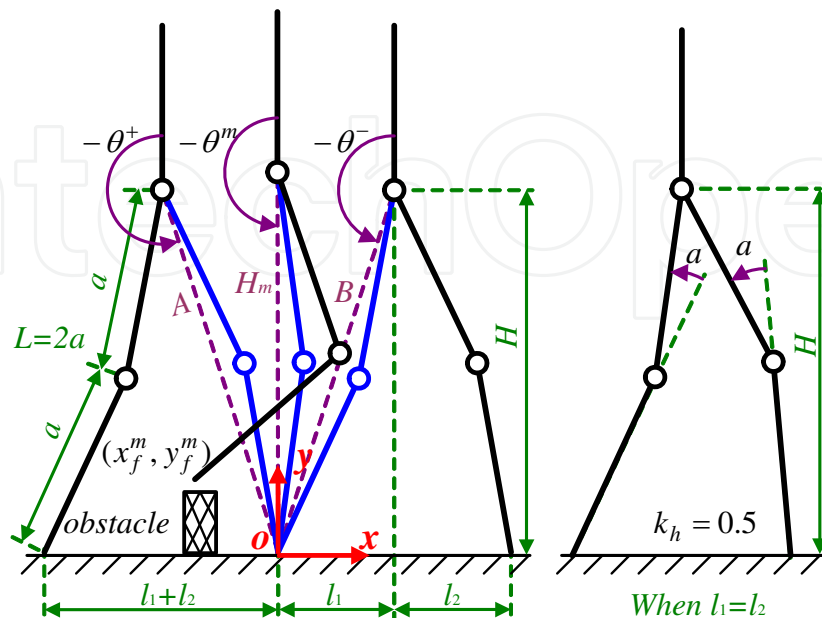
Fig. 13. Parameters of the walking pattern

Choosing

$$h_0(q) := H_0 qa \tag{38}$$

$$\theta(q) := cq \tag{39}$$

where $H_0 = \begin{bmatrix} I_{4\times4} & 0_{4\times1} \end{bmatrix}$, c = [-1 0 -1/2 0 -1].

To obtain a stable walking pattern, we propose a synthesizing method consisting of the following four steps:

1.   parameterize position constraints $h_d(\theta)$ at all breakpoints;

Since one of the basic aspects of biped locomotion is to maintain a constant erect torso, we specify q5 = 0 in the whole walking cycle, as shown in Fig. 13.

To shape the impact posture, we define two normalized non-dimensional parameters:

$$k_s := (l_1 + l_2) / L \tag{40}$$

$$k_h := l_1 / (l_1 + l_2) \tag{41}$$

where k_s describes the magnitude of the stride relative to leg length, and k_h describes the ratio of the hip abscissa to the stride. k_s and k_h could take values from 0 to 1 during normal gaits.

Let H denote the height of hip joint at impact, and. H can be determined by the following equation:

$$H = L\sqrt{\cos^2(\alpha / 2) - k_s^2 / 4} \tag{42}$$

where α is the angle of the knee joint when $k_h = 0.5$.

To be compatible with the ground condition, it is necessary to specify several middle postures to describe the swing foot over rough terrain or in environments with obstacles. For simplicity, we select one middle posture q^m where $\theta_m = (\theta^+ + \theta^-) / 2$. The height of the hip in the middle posture can be determined by $H_m = (A + B) / 2$. We utilize the Cartesian coordinates of swing foot (x_f^m, y_f^m), to parameterize q^m. The robot can negotiate different obstacles on the ground by varying (x_f^m, y_f^m).

Since both impact postures and middle postures are determined, the configuration at all breakpoints can be written as

$$h_d(\theta) = \begin{cases} H_0 q^+(k_s, k_h), & \theta = \theta^+ \\ H_0 q^m(x_f^m, y_f^m), & \theta = \theta^m \\ H_0 q^-(k_s, k_h), & \theta = \theta^- \end{cases} \tag{43}$$

2.   determine the derivative constraints $dh_d(\theta) / d\theta$ at impact postures;

Since we assume that the robot maintain a constant erect posture during the whole walking cycle, the following two conditions must be satisfied:

$$\dot{q}_5^- = 0 \tag{44}$$

$$\dot{q}_5^+ = [0_{1\times4} \quad 1]\Delta_{\dot{q}}\dot{q}^- = 0 \tag{45}$$

Observing from human walking, we find that human beings appear to hold his support knee joint and relative angle between two thighs intendedly just before impact, so we get the following equation:

$$\dot{q}_3^- = 0 \tag{46}$$

$$\dot{q}_2^- - \dot{q}_1^- = 0 \tag{47}$$

Let σ^- denote the angular momentum just before impact. According to (33), one can obtain

$$\sigma_- = -D_5(q^-)\dot{q}^- \tag{48}$$

According to equation (44) to (48), the generalized velocities $\dot{q}^-$ can be expressed as

$$\dot{q}^- = \Pi(q^-)\sigma^- \tag{49}$$

where $\Pi(q^-) = \begin{bmatrix} 0 & 0 & 0 & 0 & 1 \\ [0_{1\times4} & 1]\Delta_{\dot{q}} \\ 0 & 0 & 1 & 0 & 0 \\ & -D_5(q^-) \\ -1 & 1 & 0 & 0 & 0 \end{bmatrix}^{-1} \cdot \begin{bmatrix} 0 \\ 0 \\ 0 \\ 1 \\ 0 \end{bmatrix}$.

Considering the equation (36), the generalized velocities $\dot{q}^+$ can also be uniquely determined. Considering (38), (39), and (49), the derivative constraints at impact postures can be written as

$$\frac{dh_d}{d\theta} = \begin{cases} H_0\Pi(q^-)/(c\Pi(q^-)), & \theta = \theta^+ \\ H_0\Delta_{\dot{q}}\Pi(q^-)/(c\Delta_{\dot{q}}\Pi(q^-)), & \theta = \theta^- \end{cases} \tag{50}$$

3. obtain the continuous trajectory $h_d(\theta)$ by interpolation;

To satisfy constraint (43), (50), and the continuity conditions of the first derivative and the second derivative at all breakpoints, $h_d(\theta)$ are characterized by two third-order polynomial expressions:

$$h_d(\theta) = \begin{cases} \sum_{i=0}^{3} M_i \cdot (\theta - \theta^+)^i, & \theta \in [\theta^+, \theta^m] \\ \sum_{i=0}^{3} N_i \cdot (\theta - \theta^m)^i, & \theta \in [\theta^m, \theta^-] \end{cases} \tag{51}$$

Thereby, we can obtain M_i and N_i by third-order spline interpolation. In this way, $h_d(\theta)$ is twice differentiable during the whole single support phase. When (x_f^m, y_f^m) and α are specified, the walking pattern can be determined by the two non-dimensional parameters k_s and k_h uniquely.

4.   determine the parameters with a small section-map factor.
Considering (33), (36), (48), and (49), the section-map factor can be calculated as

$$\delta = \frac{\sigma^+}{\sigma^-} = \frac{-D_5(q^+)\dot{q}^+}{\sigma^-}$$

$$= \frac{-D_5(q^+)\Delta_{\dot{q}}\dot{q}^-}{\sigma^-} = -D_5(q^+)\Delta_{\dot{q}}(q^-)\Pi(q^-)$$

(52)

According to (52), the section-map factor only depends on q at impact. Since there are only two parameters k_s and k_h, we can easily obtain a small section-map factor by exhaustive search computation (Fu et al., 2006).

5.3 Stable walking transition and its stability analysis
According to section-map stability criterion, the robot can achieve stable walking provided that all section-map factors is less than one. Fig. 14 shows the property of angular momentum during one-step transition.
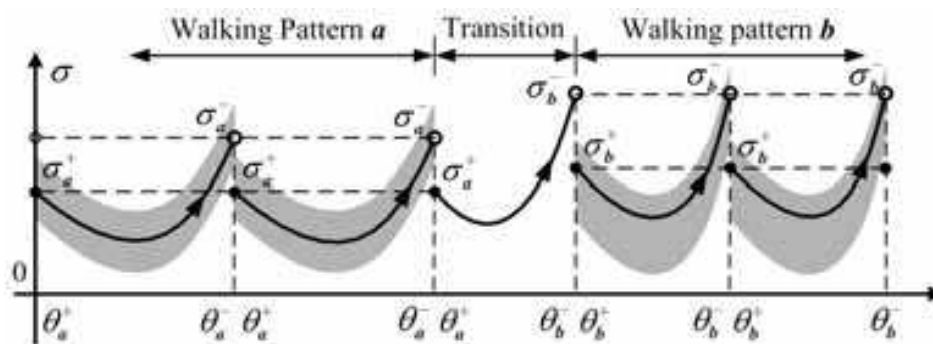
Fig. 14. Property of angular momentum during one-step transition

Moreover, each walking pattern has a domain of stable attraction, and we assume the domains before and after transition are respectively

$$a_{\min} < \sigma_a^- < a_{\max}$$

(53)

$$b_{\min} < \sigma_b^- < b_{\max}$$

(54)

Define one-step transition map $P_{a \to b} : \sigma_a^- \to \sigma_b^-$

$$P_{a \to b}(\sigma_a^-) = \sqrt{(\delta_a \cdot \sigma_a^-)^2 + 2\int_{\theta_a^+}^{\theta_b^-} I(\theta)J(\theta)d\theta}$$

(55)

To realize a stable one-step transition, the following two conditions must be satisfied:
The domain of attraction of walking pattern a can be steered into the domain of attraction of walking pattern b under transition map (Westervelt, 2003b), that is,

$$\{P_{a \to b}(\sigma_a^-) \mid a_{\min} < \sigma_a^- < a_{\max}\} \bigcap \{\sigma_b^- \mid b_{\min} < \sigma_b^- < b_{\max}\} \neq \varnothing$$

(56)

The walking with perturbation should be in the intersection set of domains:

$$\sigma_a^- \in \{\sigma_a^- \mid a_{\min} < \sigma_a^- < a_{\max}\} \bigcap \{P_{a \to b}^{-1}(\sigma_b^-) \mid b_{\min} < \sigma_b^- < b_{\max}\} \tag{57}$$

Since one-step transition map (55) is a monotonic increasing function, as shown in Fig. 15, the two stable transition conditions can be written as

$$\begin{cases} P_{a \to b}(a_{\max}) > b_{\min} \\ P_{a \to b}(a_{\min}) < b_{\max} \end{cases} \tag{58}$$

$$\min\{a_{\min}, P_{a \to b}^{-1}(b_{\min})\} < \sigma_a^- < \max\{a_{\max}, P_{a \to b}^{-1}(b_{\max})\} \tag{59}$$

Fig. 16 shows the property of angular momentum during multi-step transition, and we assume the domains before and after transition are respectively
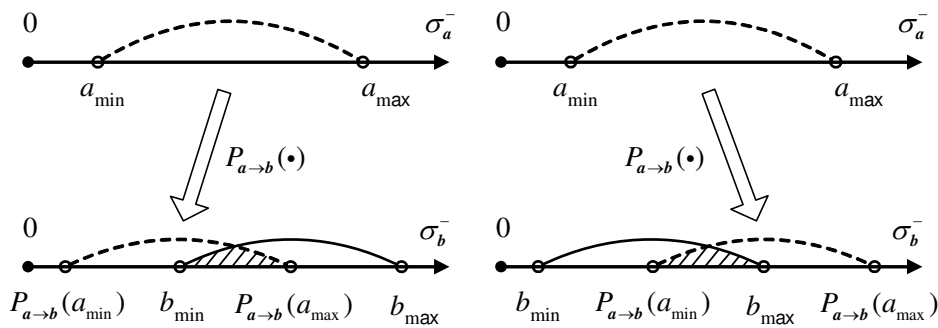
Fig. 15. Phase portraits during one-step transition

$$a_{\min} < \sigma_a^- < a_{\max} \tag{60}$$

$$d_{\min} < \sigma_d^- < d_{\max} \tag{61}$$

Define multi-step transition map $P_{a \to d} : \sigma_a^- \to \sigma_d^-$, to realize a stable multi-step transition, the following two conditions must be satisfied:

$$\{P_{a \to d}(\sigma_a^-) \mid a_{\min} < \sigma_a^- < a_{\max}\} \bigcap \{\sigma_d^- \mid d_{\min} < \sigma_d^- < d_{\max}\} \neq \varnothing \tag{62}$$

$$\sigma_a^- \in \{\sigma_a^- \mid a_{\min} < \sigma_a^- < a_{\max}\} \bigcap \{P_{a \to d}^{-1}(\sigma_d^-) \mid d_{\min} < \sigma_d^- < d_{\max}\} \tag{63}$$
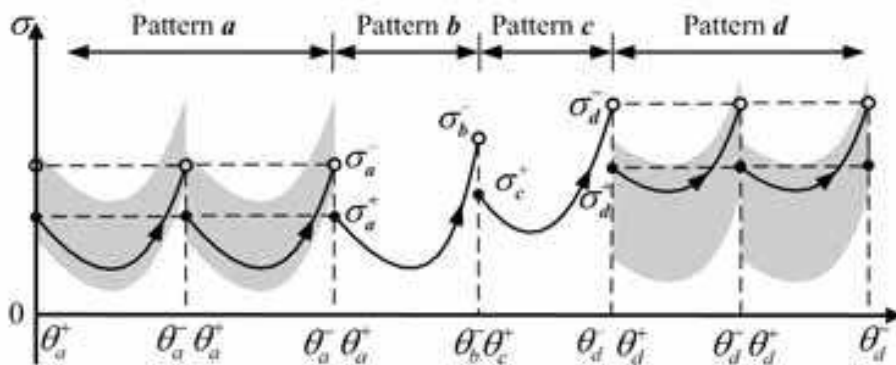
Fig. 16. Property of angular momentum during multi-step transition

6. Walking eperiments

6.1 Stable walking experiment

This section provides several experimental results toward checking the section-map stability criterion.

In the first experiment, THR-I was controlled to walk on a flat floor with a section-map factor $\delta = 0.89$. The experiment lasted more than 120s and THR-I took approximately 600 steps, which indicates the walking period is 0.2s per step. Fig. 17 gives video frames of THR-I taking four steps for a typical walking motion. Fig. 18 is the real joint angles versus time during walking. Fig. 19 are the section-map factors calculated from encoders during walking.
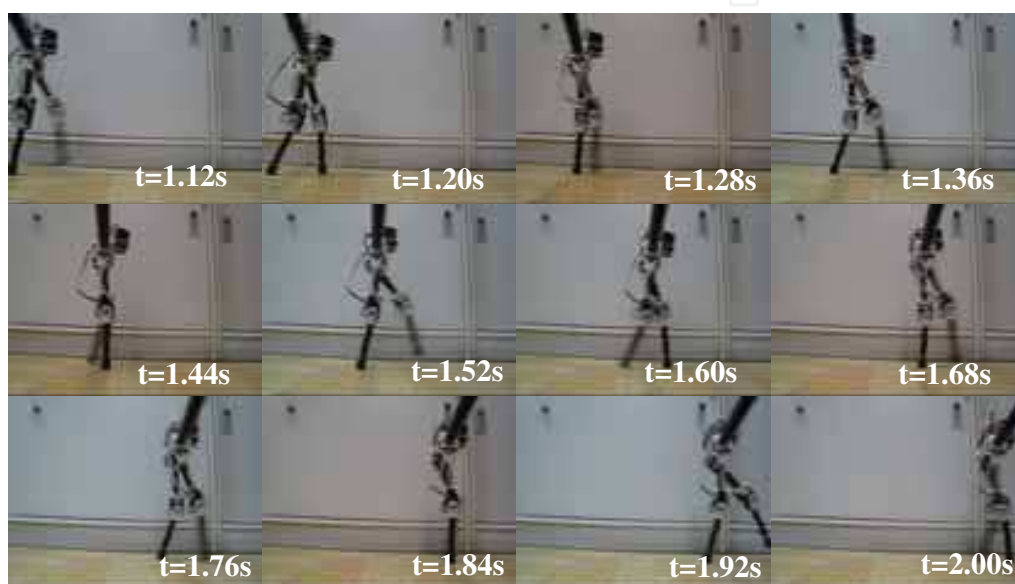
Fig. 17. Video frames of THR-I taking four consecutive steps with $\delta = 0.89$. The robot is walking at 0.20 s per step

6.2 Unstable walking experiment

The second experiment demonstrated the walking result with a section-map factor $\delta = 1.20$, which indicates the corresponding biped walking is unstable stable. Fig. 20 shows the desired and real values of holonomic constraints, from which we can observe that the walking pattern can not be imposed on the robot. Fig. 21 is the corresponding snapshot of the walking experiment, from which one can see the robot falls forward finally.

For periodic forward walking, the minimum of the angular momentum around the pivot point during a walking cycle should be positive; otherwise the robot has no enough energy to achieve a step and will fall backward. Fig. 22 is the desired and real values of holonomic constraints during walking on level ground with the section factor $\sigma_{\min} < 0$, which indicates that the robot will fall backward finally. Fig. 23 is the snapshot of walking experiment.

6.3 Stable walking transition experiment

The fourth experiment demonstrated the walking transition. Fig. 24 is simulation results of phase portraits during one-step transition with a 5% error from limit cycles before

transition. The section-map factor before transition is 0.86, and after transition is 0.89; therefore, the walking is stable. Fig. 25 gives video frames of THR-I walking from 0.2s/step to 0.3s/step.
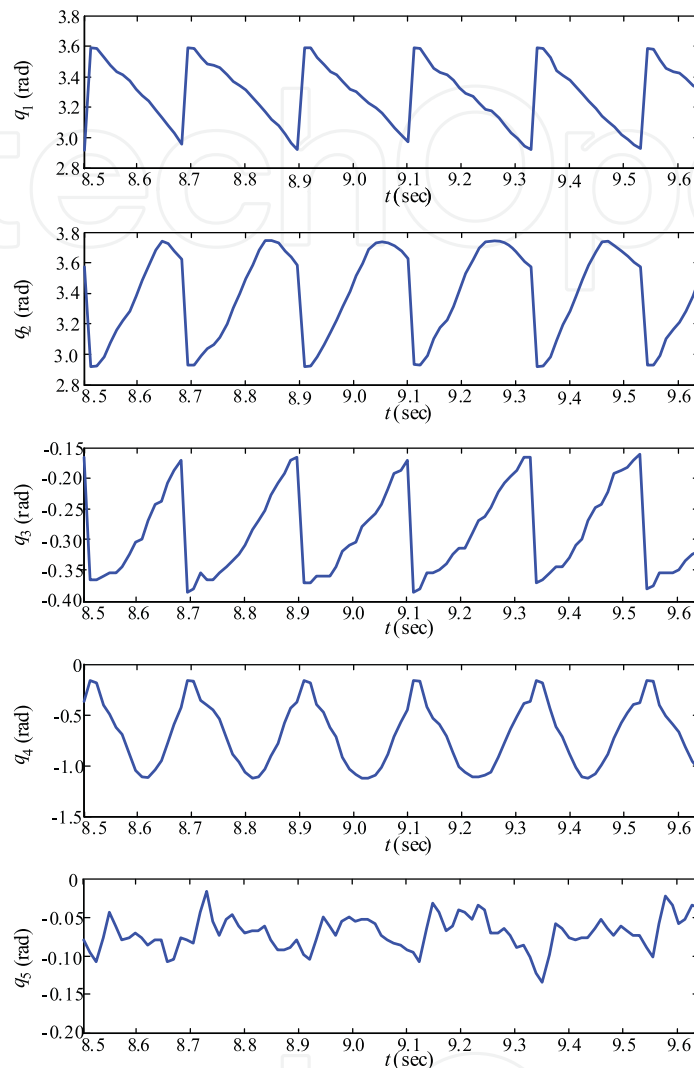

Fig. 18. Real joint angles of THR-I with $\delta = 0.89$
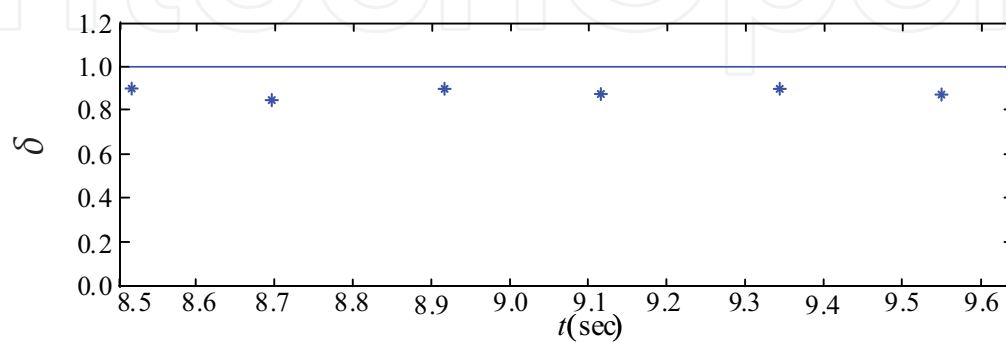
Fig. 19. Section-map factor estimated by rotary encoders during walking. All section-map factors are.less than one
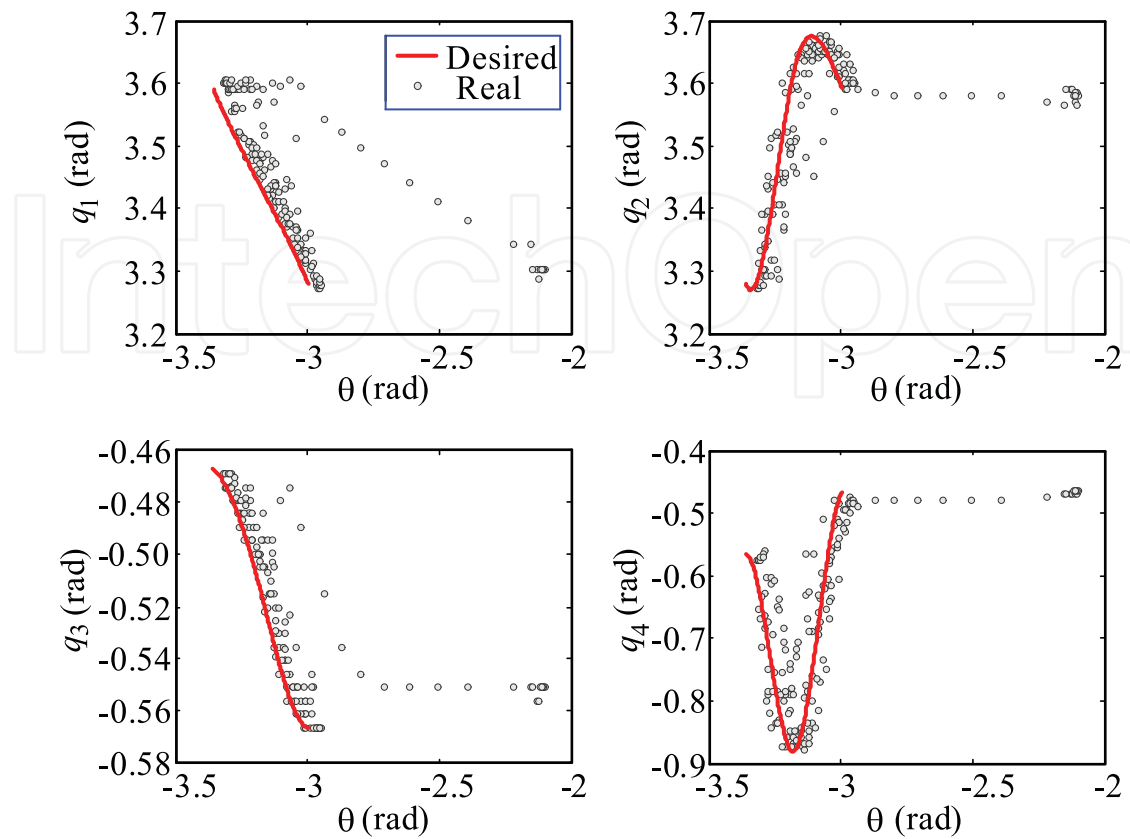
Fig. 20. Desired and real values of holonomic constraints with $\delta = 1.2$
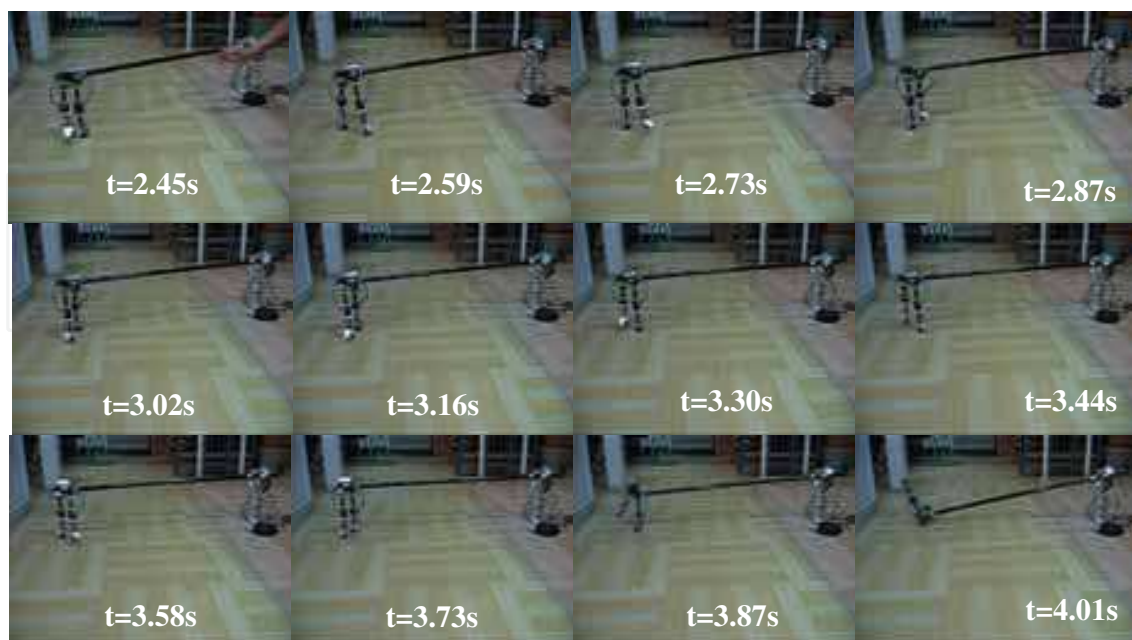
Fig. 21. Video frames of biped walking experiment with $\delta = 1.2$
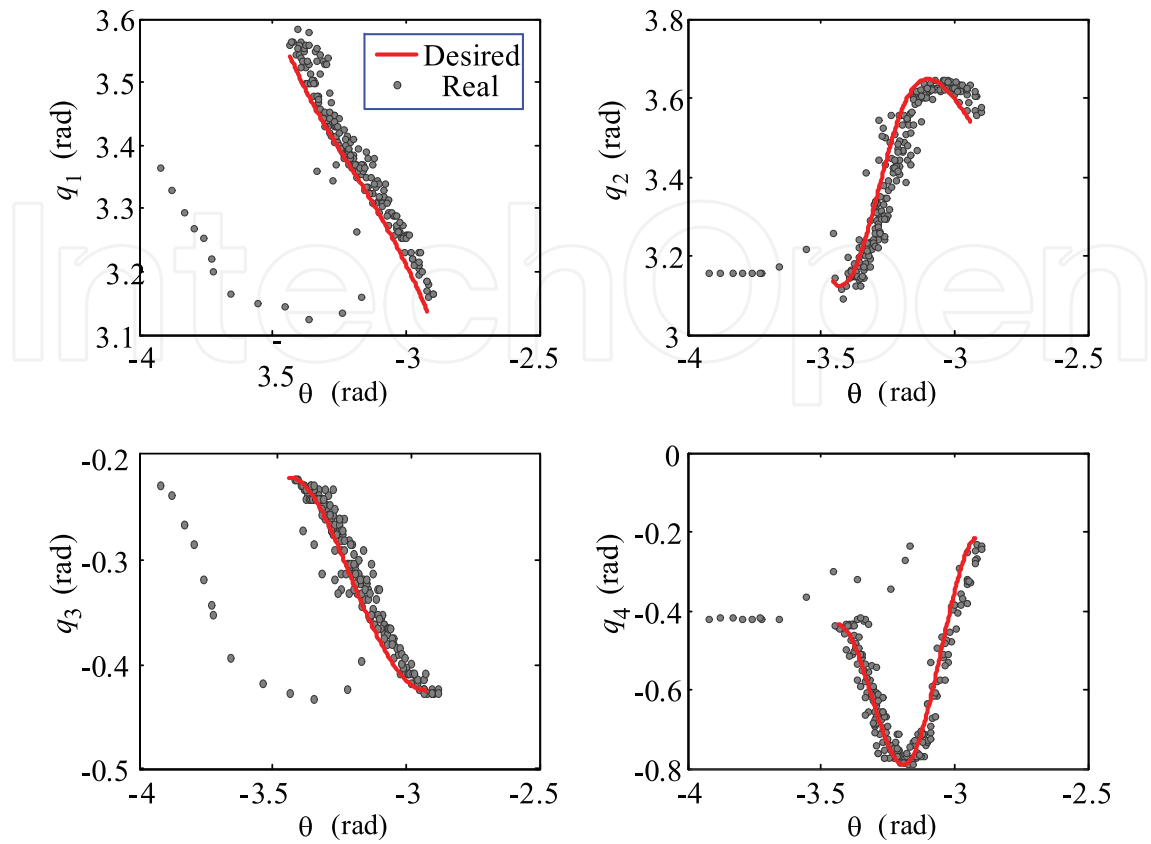
Fig. 22. Desired and real values of holonomic constraints with $\sigma_{\min} < 0$
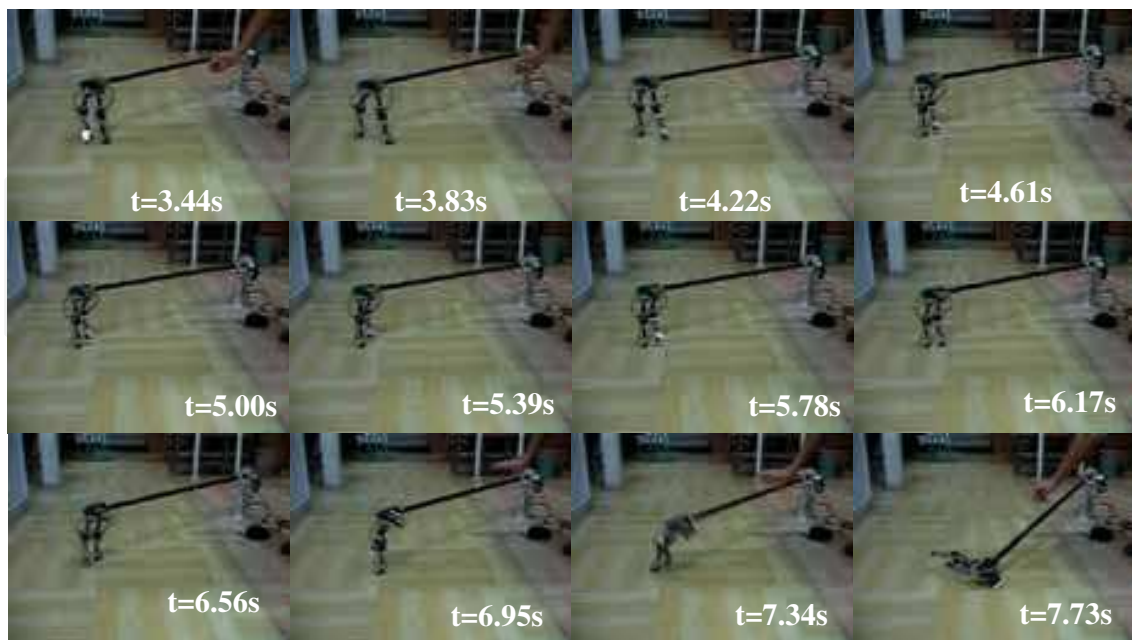
Fig. 23. Video frames of biped walking experiment with $\sigma_{\min} < 0$
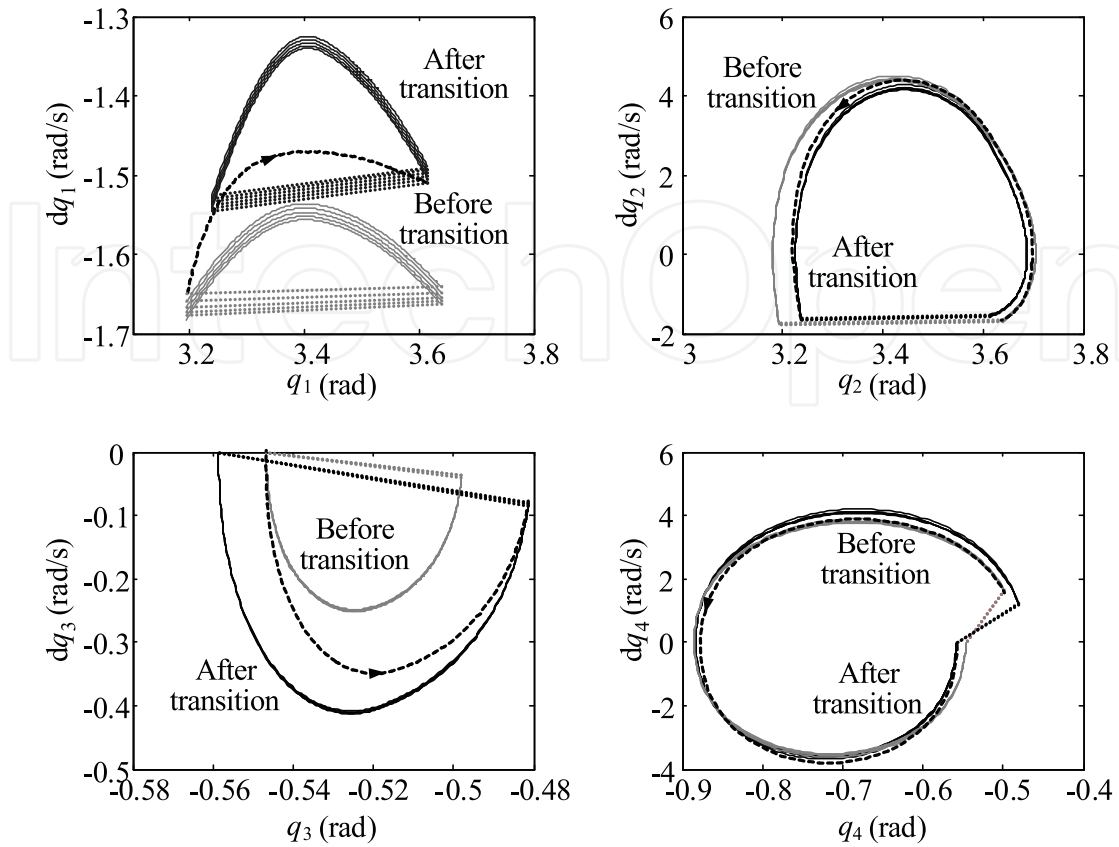
Fig. 24. Simulation results of phase portraits during one-step transition
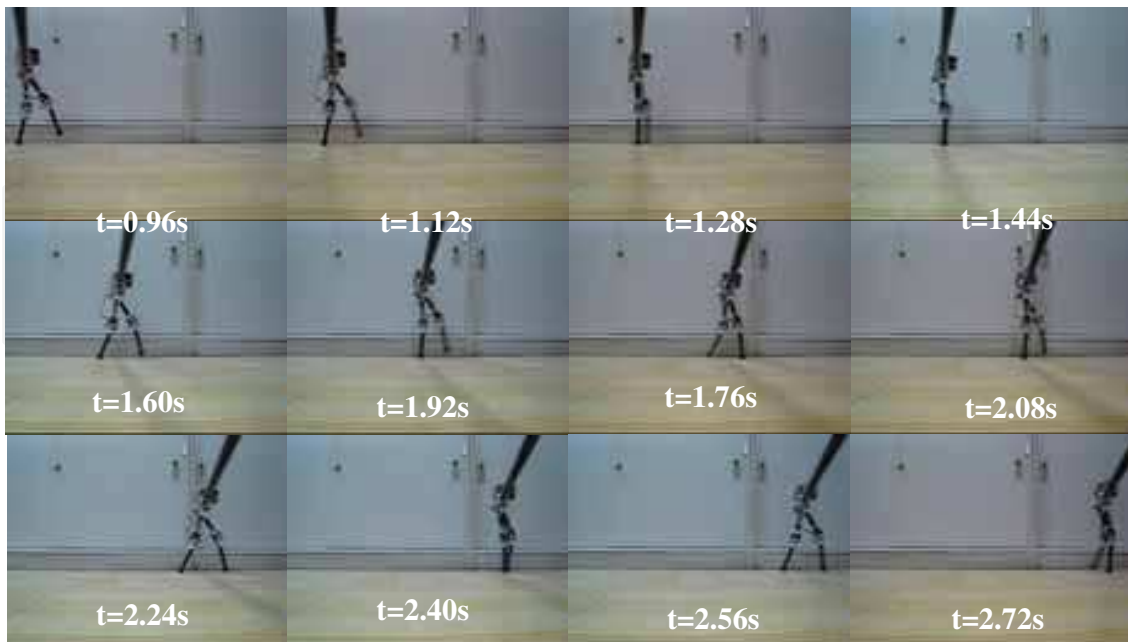
Fig. 25. Video frames of biped walking transition experiment

7. Conclusion

When publications are referred in the text, enclose the author's name and the date of publication within the brackets. For one author, use author's surname and the date (Arkin, 2004). For two authors, give both names & the year (Mataric & Brooks, 1999). For three or more authors, use the first author, plus „et al.", and the date (Siegwart et al., 2006). If giving a list of reference, separate them using semicolons.

In this study, we focused on a coherent stability criterion and its application methods for biped walking. The main results of this chapter are summarized as follows:

1. An overall mathematical modelling method for biped walking is proposed based on dimension-variant hybrid automata. This method expresses the overall biped walking model as an 8-tuple and can reflect all kinds of continuous and discrete properties of biped walking, which makes it possible to study stability and design control strategy for biped locomotion from a global point of view.

2. A rigorous mathematical definition of biped walking stability is presented by combining the character of biped locomotion with the notion of classical stability from the view of hybrid trajectory. It is pointed out that the model in the task space is a length-varying and inertia-varying inverted pendulum, and the analytic form of the inverted pendulum model is derived. This makes it possible to study stability of biped walking in a low-dimension task space.

3. It is pointed out that, under some assumption, stability of the hybrid trajectory is equivalent to that of the section sequence at switch section in the task space of biped walking. Based on this result, section-map stability criterion is presented. This criterion is applicable not only to dynamic walking which ZMP criterion can not solve, but also to non-periodic walking which Poincare return map criterion can not solve.

4. By the proposed criterion, a synthesizing method for walking patterns based on section-map factor is presented. The effectiveness of this method is confirmed by a biped robot THR-I, which can walk with a relative speed of 2 leg lengths per second. This robot is one of the few biped machines which can walk so fast and stable (Geng et al., 2006).

Since the sagittal plane dynamics of biped walking are almost decoupled from those in the frontal plane (Furusho & Sano, 1990; Kuo, 1999), this chapter is only concentrated on stability issue in sagittal plane. The future work is to extend this method to the frontal plane to produce stable, dynamic three-dimensional walking.

8. References

Canudas-de-Wit, C. (2004). On the concept of virtual constraints as a tool for walking robot control and balancing. *Annual Reviews in Control*, Vol. 28, No. 2, 157-166

Chevallereau, C.; Abba, G.; Aoustin, Y. ; Plestan, F. ; Westervelt, E. R.; Canudas-de-wit, C.; & Grizzle, J. W. (2003). RABBIT: A testbed for advanced control theory. *IEEE Contr. Syst. Mag.*, Vol. 23, No. 5, 57-79

Chevallereau, C.; Formal'sky, A. & Djoudi, D. (2004). Tracking of a joint path for the walking of an underactuated biped. *Robotica*, Vol. 22, No. 1, 15-28

Fu, C.; Shuai, M.; Huang, Y.; Wang, J. & Chen, K. (2006). Parametric walking patterns and optimum atlases for underactuated biped robots, *Proc. IEEE Int. Conf. Intell. Robots Syst.*, 342-347

Furusho, J. & Sano, A. (1990). Sensor-based control of a nine-link biped. *Int. J Robot. Res.*, Vol. 9, No. 2, 83-98

Geng, T.; Porr, B. & Worgotter, F. (2006). Fast biped walking with a sensor-driven neuronal controller and real-time online learning. *Int. J Robot. Res.*, Vol. 25, No. 3, 243-259

Goswami, A.; Espiau, B. & Keramane, A. (1996). Limit cycles and their stability in a passive bipedal gait," in Proc. IEEE Int. Conf. Robot. Autom., 246-251

Goswami, A. & Kallem, V. (2004). Rate of change angular momentum and balance maintenance of biped robots, *Proc. IEEE Int. Conf. Robot. Autom.*, 3785-3790

Grizzle, J. W.; Abba, G. & Plestan, F. (2001). Asymptotically stable walking for biped robots: Analysis via systems with impulse effects. *IEEE Trans. Autom. Contr.*, Vol. 46, No. 1, 51-64

Guckenheimer, J. & Holmes, P. (1985). *Nonlinear Oscillations, Dynamical Systems, and Bifurcations of Vector Fields*. New York: Springer-Verlag

Hirai, K.; Hirose, M.; Haikawa, Y. & Takenaka, T. (1998). The development of Honda humanoid robot, *Proc. IEEE Int. Conf. Robot. Autom.*, 1321-1326

Huang, Q. ; Yokoi, K.; Kajita, S.; Kaneko, K.; Arai, H.; Koyachi, N. & Tanie, K. (2001). Planning walking patterns for a biped robot. *IEEE Trans. Robot. Autom.*, Vol. 17, No.3, 280-289

Huang, Q. & Nakamura, Y. (2005). Sensory reflex control for humanoid walking. *IEEE Trans. Robot. Autom.*, Vol. 21, No. 5, 977-984

Hurmuzlu, Y. &Moskowitz, G. Bipedal locomotion stabilized by impact and switching. (1993). *Dyn. Stab. Syst.*, Vol. 60, No. 2, 331-344

Kajita, S.; Matsumoto, O. & Saigo, M. (2001). Real-time 3-D walking pattern generation for a biped robot with telescopic legs, Proc. *IEEE Int. Conf. Robot. Autom.*, 2299-2306.

Kuo, A. D. (1999). Stabilization of lateral motion in passive dynamic walking. *Int. J Robot. Res.*, Vol. 18, No. 9, 917-930

Kuo, A. D. (2002). Energetics of actively powered locomotion using the simplest walking model. *Journal of Biomechanical Engineering*, Vol. 124, 113-120

Lim, H.; Kaneshima, & Takanishi, Y. (2002). A. On-line walking pattern generation for biped humanoid robot with trunk, *Proc. IEEE Int. Conf. Robot. Autom.*, 3111-3116

McGeer, T. (1990). Passive walking with knees, *Proc. IEEE Int. Conf. Robot. Autom.*, 1990, 1640-1645

Nishiwaki, K.; Kagami, S.; Kuniyoshi, Y.; Inaba, M. &Inoue, H. (2002). Online generation of humanoid walking motion based on fast generation method of motion pattern that follows desired ZMP, *Proc. IEEE Int. Conf. Intell. Robots Syst.*, 2684-2689

Popovic, M. & Englehart, A. (2004). Angular momentum primitives for human walking: biomechanics and control, *Proc. IEEE Int. Conf. Intell. Robots Syst.*, 1658-1691

Pratt, J. & Tedrake, R. (2005). Velocity based stability margins for fast bipedal walking, *Proc. 1st Ruperto Carola Symp. Fast Motions in Biom. and Robot.*, 1-27

Raibert, M. H. (1986). *Legged robots that balance*. MIT Press, Cambridge, MA

Takanishi, A.; Ishida, M.; Yamazaki, Y. &Kato, I. (1985). The realization of dynamic walking robot WL-10RD, *Proc. Int. Conf. Adv. Robot.*, 459-466

Vukobratovic, M. & Juricic, D. (1969). Contribution to the synthesis of biped gait. *IEEE Trans. Biomed. Eng.*, Vol. BME-16, No. 1, 1-6

Westervelt, E. R.; Grizzle, J. W. & Koditschek, D. (2003a). Hybrid zero dynamics of planar biped walkers. I*EEE Trans. Autom. Contr.*, Vol. 48, No. 1, 42-56

Westervelt, E. R.; Grizzle, J. W. & Canudas-de-Wit, C. (2003b). Switching and PI control of walking motions of planar biped walkers. *IEEE Trans. Autom. Contr.*, Vol. 48, No. 2, 308-312
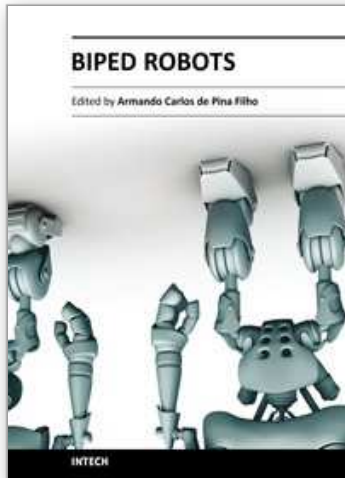
Biped Robots

Edited by Prof. Armando Carlos Pina Filho

Biped robots represent a very interesting research subject, with several particularities and scope topics, such as: mechanical design, gait simulation, patterns generation, kinematics, dynamics, equilibrium, stability, kinds of control, adaptability, biomechanics, cybernetics, and rehabilitation technologies. We have diverse problems related to these topics, making the study of biped robots a very complex subject, and many times the results of researches are not totally satisfactory. However, with scientific and technological advances, based on theoretical and experimental works, many researchers have collaborated in the evolution of the biped robots design, looking for to develop autonomous systems, as well as to help in rehabilitation technologies of human beings. Thus, this book intends to present some works related to the study of biped robots, developed by researchers worldwide.

How to reference

In order to correctly reference this scholarly work, feel free to copy and paste the following:

INTECH
open science | open minds